

# Characterization of Mechanical and Physical Properties of Silica Aerogels Using Molecular Dynamics Simulation

Jingjie Yeo<sup>1</sup>, Jincheng Lei<sup>2</sup>, Zishun Liu<sup>2,\*</sup>, Teng Yong Ng<sup>1</sup>

<sup>1</sup> School of Mechanical and Aerospace Engineering, Nanyang Technological University, 50 Nanyang Avenue, 639798 (Singapore)

<sup>2</sup> International Centre for Applied Mechanics, State Key Laboratory for Strength and Vibration of Mechanical Structures, Xi'an Jiaotong University, Xi'an, 710049, China

\* Corresponding author: zishunliu@mail.xjtu.edu.cn

---

**Abstract** Silica aerogels are nanoporous ultralight materials with extreme materials properties: the highest specific surface area of any material; slowest speed of sound through any solid material; excellent thermal insulators. Using molecular dynamics and the Tersoff potential, re-parameterized to simulate silicon dioxide, we have modeled the porous structures of silica aerogels. Our study shows that this potential is more suitable for modeling thermal properties in amorphous silica than the widely-used BKS potential. Increasing densities of aerogel samples are generated using an expanding and quenching process. Analysis of the fractal dimensions indicates a good fit with previous theoretical and experimental results. Each sample's thermal conductivity is determined using reverse non-equilibrium molecular dynamics. Results indicate that the power-law fit of our data reflects the power-law exponent found in experimental studies. The results are also of the same order of magnitude as experimental bulk aerogel, but they are consistently higher. Analysis of the pore size distribution shows, firstly, that such a disparity is due to limited pore sizes represented in a finite nano-sized system, and secondly, that increasing system length scales leads to corresponding increases in the pore sizes that can be represented. Furthermore, we attempt to determine the mechanical properties, such as Young's modulus of aerogel by using the same potential. We can conclude from all these results that our model is very suitable for modeling the mechanical and physical properties of bulk silica aerogel, and that an appropriate system length scale can be chosen to suit the pore size regime of interest.

**Keywords** molecular dynamics, silica aerogel, nanoporous ultralight materials.

---

## 1. Introduction

Silica aerogel is an exceptionally percolated material [1], made from various sol-gel processes and supercritical drying. Some silica aerogel's properties include very low density and extremely high thermal resistance [2, 3]. Previous experimental studies characterized silica aerogel's thermal conductivity and transport mechanisms, and found that the solid thermal conductivity scaled with density via a power law:

$$\lambda_s = C\rho^\alpha \quad (1)$$

where  $\alpha$  was approximately 1.6 for densities between 0.3 to 1.0g/cm<sup>3</sup> [4]. Previous numerical studies characterizing the properties of silica aerogel [5, 6] include accurate reproductions of the porous and fractal nature of silica aerogels [7-9]. Murillo *et al.* [9] devised an expanding, heating and quenching method to model silica aerogels, obtaining good fits for the elastic moduli in comparison with experimental results. Ng *et al.* [6] employed negative pressure rupturing with the van Beest, Kramer and van Santen (BKS) potential [10, 11], and determined their thermal conductivities. It was found that the power-law fit of the data corresponds to experimental bulk sintered aerogel.

In this study, new methods are used to attain a closer fit of the thermal conductivity, in comparison with experimental data. We have found that the Tersoff potential, re-parameterized to model silicon dioxide, is more suitable than the BKS potential in predicting the thermal conductivity of amorphous silica. The solid thermal conductivity of silica aerogels are determined using reverse non-equilibrium MD (RNEMD) simulations, by generating the porous samples using the method by

Murillo et al. [9] and obtaining aerogel densities in the range of 0.3 to 1.0g/cm<sup>3</sup>. The results are plotted and compared against experimental data [4]. The mechanical property, such as Young's modulus is simulated by using same method. The Young's modulus of aerogel with densities in the range of 0.3 to 1.0g/cm<sup>3</sup> is presented also.

## 2. Simulation Methods

The simulations are performed on the LAMMPS [12] software. The interaction potential used is the Tersoff potential [13], re-parameterized to model interactions between silicon and oxygen [14]. From comparison studies using the BKS potential and Tersoff potential, it is found that the Tersoff potential is more suitable for thermal conductivity studies. , while, the BKS potential augmented with a “24-6” Lennard Jones potential can prevent uncontrollable dynamics at very high temperatures [15]. Using the method by Murillo *et al.* [9], porous aerogel structures can be formed by expanding, heating and quenching, producing aerogels in the density range of 0.3 to 1.0g/cm<sup>3</sup>. RNEMD [6, 16-18] can be used to determine the thermal conductivity at each aerogel density, where energies are swapped once every 0.025ps, while the system is kept an average temperature of 300K. This amount of swapping ensures a rapid convergence of the simulated temperature gradient, and produced a linear response within the simulation cell. The system is allowed to equilibrate for a further 1.0ns till a fully linear response has been obtained, and finally, the temperature gradient is averaged over another 50ps. The total solid thermal conductivity can be found by averaging over 5 independent samples at each density. To investigate the Young's modulus with the strain rate 0.0005ps<sup>-1</sup> for 200ps, the tension tests are carried out on samples of different densities.

## 3. Results and Discussions

### 3.1. Thermal conductivity of dense amorphous silica

The thermal conductivity of increasing lengths of amorphous silica is compared with experimental results to validate our MD scheme. These amorphous silica samples are generated by quenching  $\beta$ -cristobalite, from 5000K to 300K. Their thermal conductivities are determined, as shown in Fig. 1 with their error bars.

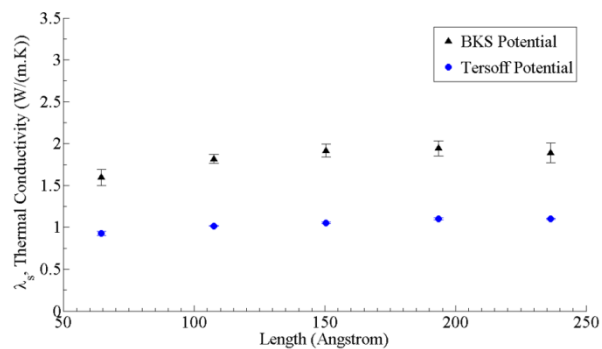


Figure 1. Amorphous silica of various lengths and their thermal conductivities

As the system length increases, so do the thermal conductivity, such that the BKS potential significantly overshoots the thermal conductivity of bulk amorphous silica, which lies between 1.37 – 1.4W/(m.K) [19]. The Tersoff potential plateaus at 1.10 ± 0.01W/(m.K) shows an almost linear dependence with increasing length scales. By extrapolating the results to an infinite length scale, thus representing bulk amorphous silica, the Tersoff potential can give a much better estimation of bulk thermal properties. The inverse of the thermal conductivities versus the inverse of the lengths

$(1/\lambda_s$  vs  $1/L$ ) are plotted and extrapolated in Fig. 2.

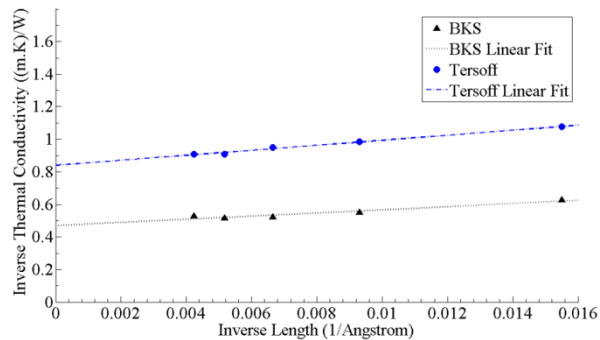


Figure 2. The inverse of the thermal conductivities for amorphous silica systems and their linear extrapolation to infinite lengths

This method gives values of 2.13W/(m.K) for the BKS potential, and 1.19W/(m.K) for the Tersoff potential, at bulk length scales. This gives an error of 55% overestimation for the former, and 13% underestimation for the latter, clearly showing that the re-parameterized Tersoff is much more capable of reproducing bulk thermal properties than the BKS potential can. This is analyzed further by examination of the vibrational density of states (vDOS) of each potential, as shown in Fig. 3, which are obtained through the discrete Fourier transform of the velocity autocorrelation function (VACF) [20].

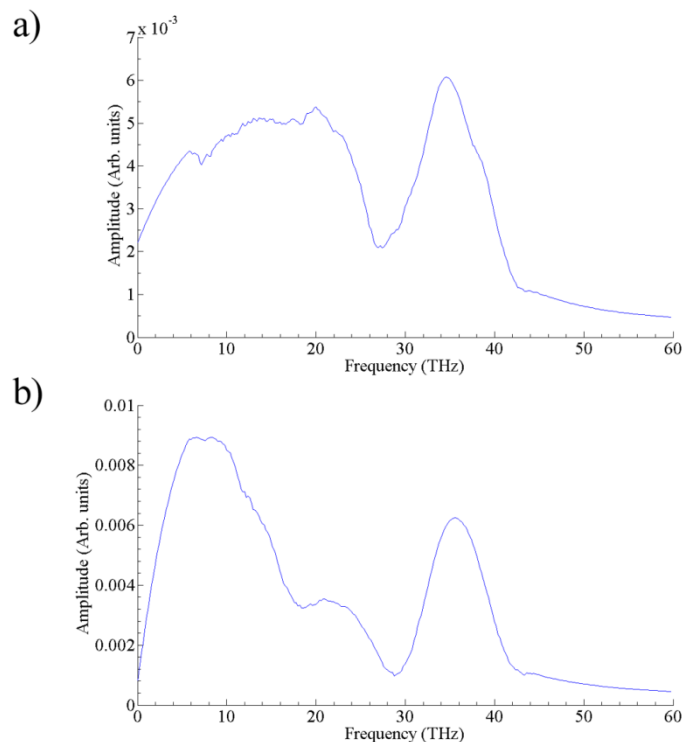


Figure 3. vDos of a) BKS, and b) Tersoff potential

The Tersoff potential clearly shows, as shown in Fig. 6b, the same peaks near the frequencies of 10.5THz, 24.0THz and 36.0THz determined from previous experimental and theoretical results by Laughlin *et al.* [21]. However, the BKS potential, in Fig. 6a, shows no apparent peaks below the 30THz region. Thus, from all these methods presented, we can conclude that the re-parameterized Tersoff potential is a far superior alternative in the thermal characterization of bulk amorphous

silica than the BKS potential.

### 3.2. Structural correlations of porous silica aerogel

Using the method discussed in Section 2, percolated silica aerogel was simulated on a cubic system of 52,728 atoms, with densities ranging from 0.3 to 1g/cm<sup>3</sup>. Fractal dimensions are determined using the method proposed by Kieffer *et al.* [7], where the total radial distributions for each density are calculated, and power-law decays are superimposed on the peak structures to determine the fractal dimensions. These results are plotted in Fig. 4 below along with their error bars, as well as data from previous theoretical studies by Murillo *et al.* [9].

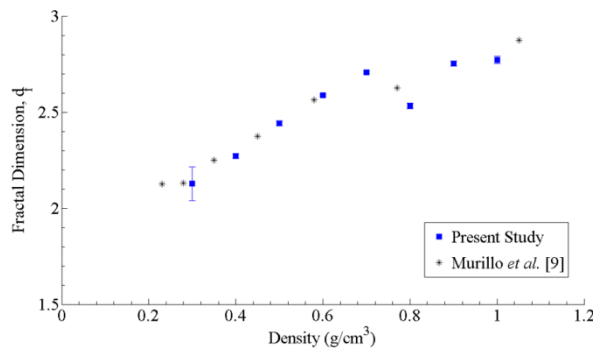


Figure 4. Decreasing fractal dimensions as density decreased

The variation of the fractal dimension,  $d_f$ , with density agrees with those found in previous theoretical and experimental studies. Experimental silica aerogel fractal dimensions varies with processing conditions, where it is approximately 1.8 under basic processing conditions, and about 2.2 to 2.4 in both acidic and neutral conditions [22].

### 3.3. Thermal conductivity of porous silica aerogel

Fig. 5 shows the data obtained, from RNEMD, as a log-scale plot with their corresponding errorbars, and the power-law fit of the data.

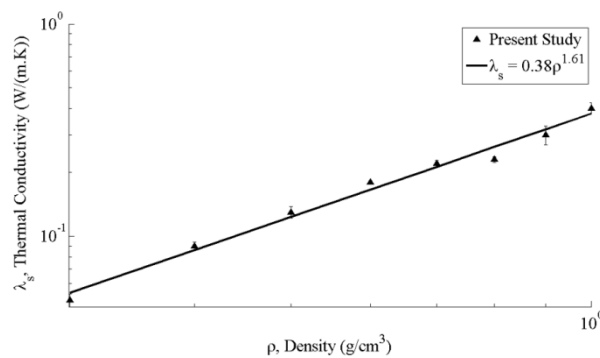


Figure 5. Log-scale plot of the power-law variation of thermal conductivity with density

Thermal conductivity is found to decrease as density decreases, in a non-linear fashion. At the lowest density of 0.3g/cm<sup>3</sup>, the thermal conductivity also reaches its lowest value of 0.05 ± 0.003W/(m.K). The power-law exponent,  $\alpha$ , of experimental bulk aerogel was found to be 1.6 in the density range of 0.3 to 1.0g/cm<sup>3</sup> [4]. Our results show an  $\alpha$  value of 1.61 in this density range, correlating very well with experimental results. Our model is also advantageous in that very low densities are achievable, much lower than 0.1g/cm<sup>3</sup>, without any adverse phenomena. A downside

of our current model is that thermal conductivities at each density were 5 times higher than experimental aerogels. The most significant reason is that our model is unable to attain micropores. This can be seen in the pore size distribution of samples of increasing aerogel length scales. Shown in Fig. 6, these plots are calculated using PSDsolv [23], which determines the relative probability of finding pores of different sizes. At a density of  $0.3\text{g/cm}^3$ , we generate two different samples with system lengths of  $180\text{\AA}$  (our current system length at  $0.3\text{g/cm}^3$ ), and  $277\text{\AA}$ .

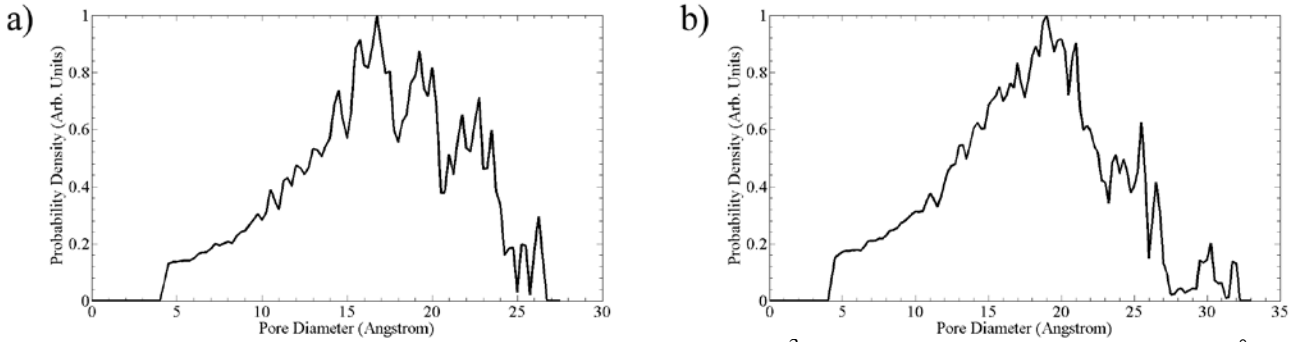


Figure 6. Pore size distribution (PSD) at density of  $0.3\text{g/cm}^3$ , at system length scales of a)  $180\text{\AA}$ , and b)  $277\text{\AA}$

The largest pore sizes accessible increase from  $27.5\text{\AA}$  to  $32\text{\AA}$  in diameter, as the system length scales increase. The pore sizes attainable are nowhere near the micron-sized diameters in bulk experimental silica aerogels.

### 3.4. Young’s modulus

Using the method discussed in Section 2, the Young’s modulus of silica aerogel with different densities ranging from  $0.3\text{g/cm}^3$  to  $1.0\text{g/cm}^3$  are obtained through MD simulation as shown in Fig. 7. A power-law fit can be used to describe the relationship between Young’s modulus and density of samples [9]. From Fig. 7, the exponent of the relationship between Young’s modulus and density can be obtained and the exponent value is about 2.4313. This value has slightly difference with the result from Murillo *et al.* [9] which was 3.11, while the magnitude of the constant of Young’s modulus is almost the same. The discrepancy mainly results from the different interactive potential.

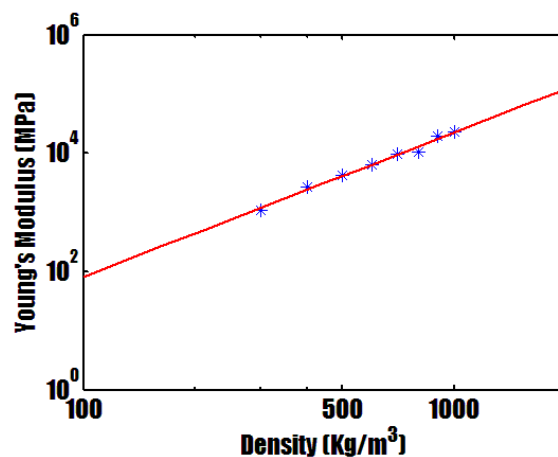


Figure 7. Relation between Young’s Modulus and density. (Red line refers to the power-law fitting line, and the blue dots refers to the simulation data.)

## 4. Conclusions

We have used MD and the re-parameterized Tersoff potential to model the porous structures of silica aerogels. We demonstrate that this potential is suitable for modeling thermal properties in amorphous silica. Using a quenching and expanding process, different densities of aerogel samples are generated. Good fits with previous results are obtained when the fractal dimensions are analyzed. Through RNEMD, their thermal conductivity is determined and the power-law fit of our data corresponds well with experimental studies. Thermal conductivities are also consistently higher than experimental bulk aerogel and analysis of the pore size distribution shows limited pore sizes could be the key issue here.

## Acknowledgements

This work is supported by the Agency for Science, Technology and Research (A\*STAR), Republic of Singapore. The authors thank the staff in A\*STAR Computational Resource Centre for providing valuable technical support. ZS and JC are also grateful for the support from the National Natural Science Foundation of China through grant number 11242011 and number 11021202.

## References

- [1] S.S. Kistler, Coherent expanded aerogels and jellies. *Nature*, 127 (1931) 741-741.
- [2] J. Fricke, SiO<sub>2</sub>-Aerogels - Modifications and Applications. *J Non-Cryst Solids*, 121 (1990) 188-192.
- [3] N. Hüsing, U. Schubert, Aerogels - Airy Materials: Chemistry, Structure, and Properties. *Angewandte Chemie - International Edition*, 37 (1998) 22-45.
- [4] J. Fricke, Aerogels - Highly Tenuous Solids with Fascinating Properties. *J Non-Cryst Solids*, 100 (1988) 169-173.
- [5] L.D. Gelb, Simulation and Modeling of Aerogels Using Atomistic and Mesoscale Methods, in: M.A. Aegerter, N. Leventis, and M.M. Koebel (Eds.), *Aerogels Handbook*, Springer, New York, 2011, pp. 565-581.
- [6] T.Y. Ng, J.J. Yeo, Z.S. Liu, A molecular dynamics study of the thermal conductivity of nanoporous silica aerogel, obtained through negative pressure rupturing. *J Non-Cryst Solids*, 358 (2012) 1350-1355.
- [7] J. Kieffer, C.A. Angell, Generation of Fractal Structures by Negative-Pressure Rupturing of SiO<sub>2</sub> Glass. *J Non-Cryst Solids*, 106 (1988) 336-342.
- [8] A. Nakano, L.S. Bi, R.K. Kalia, P. Vashishta, Molecular-Dynamics Study of the Structural Correlation of Porous Silica with Use of a Parallel Computer. *Phys Rev B*, 49 (1994) 9441-9452.
- [9] J.S.R. Murillo, M.E. Bachlechner, F.A. Campo, E.J. Barbero, Structure and mechanical properties of silica aerogels and xerogels modeled by molecular dynamics simulation. *J Non-Cryst Solids*, 356 (2010) 1325-1331.
- [10] B.W. van Beest, G.J. Kramer, R.A. van Santen, Force fields for silicas and aluminophosphates based on ab initio calculations. *Phys Rev Lett*, 64 (1990) 1955-1958.
- [11] G.J. Kramer, N.P. Farragher, B.W. van Beest, R.A. van Santen, Interatomic force fields for silicas, aluminophosphates, and zeolites: Derivation based on ab initio calculations. *Phys Rev B Condens Matter*, 43 (1991) 5068-5080.
- [12] S. Plimpton, Fast Parallel Algorithms for Short-Range Molecular-Dynamics. *J Comput Phys*, 117 (1995) 1-19.
- [13] J. Tersoff, Modeling solid-state chemistry: Interatomic potentials for multicomponent systems.

- Phys Rev B, 39 (1989) 5566-5568.
- [14] S. Munetoh, T. Motooka, K. Moriguchi, A. Shintani, Interatomic potential for Si-O systems using Tersoff parameterization. *Computational Materials Science*, 39 (2007) 334-339.
  - [15] A.J.H. McGaughey, M. Kaviani, Thermal conductivity decomposition and analysis using molecular dynamics simulations Part II. Complex silica structures. *Int J Heat Mass Tran*, 47 (2004) 1799-1816.
  - [16] F. Muller-Plathe, P. Bordat, Reverse non-equilibrium molecular dynamics. *Lect Notes Phys*, 640 (2004) 310-326.
  - [17] T.Y. Ng, J.J. Yeo, Z.S. Liu, A molecular dynamics study of the thermal conductivity of graphene nanoribbons containing dispersed Stone–Thrower–Wales defects. *Carbon*, 50 (2012) 4887-4893.
  - [18] J.J. Yeo, Z.S. Liu, T.Y. Ng, Comparing the effects of dispersed Stone–Thrower–Wales defects and double vacancies on the thermal conductivity of graphene nanoribbons. *Nanotechnology*, 23 (2012) 385702.
  - [19] M.J. Weber, Glasses, in: *Handbook of Optical Materials*, CRC Press, Boca Raton, Florida, 2002.
  - [20] M.T. Dove, *Introduction to Lattice Dynamics*, Cambridge University Press, Cambridge, 1993.
  - [21] R.B. Laughlin, J.D. Joannopoulos, Phonons in amorphous silica. *Phys Rev B*, 16 (1977) 2942-2952.
  - [22] T. Woignier, J. Phalippou, R. Vacher, J. Pelous, E. Courtens, Different kinds of fractal structures in silica aerogels. *J Non-Cryst Solids*, 121 (1990) 198-201.
  - [23] S. Bhattacharya, K.E. Gubbins, Fast Method for Computing Pore Size Distributions of Model Materials. *Langmuir*, 22 (2006) 7726-7731.